

Expansion of the Decoupled Discrete-Time Jacobian Eigenvalue Approximation for Model-Free Analysis of PMU Data

Sean D. Kantra, Elham B. Makram

Holcombe Department of Electrical and Computer Engineering, Clemson University, Clemson, USA

Email: skantra@g.clemson.edu, makram@clemson.edu

How to cite this paper: Kantra, S.D. and Makram, E.B. (2017) Expansion of the Decoupled Discrete-Time Jacobian Eigenvalue Approximation for Model-Free Analysis of PMU Data. *Journal of Power and Energy Engineering*, 5, 14-35.
<https://doi.org/10.4236/jpee.2017.56002>

Received: May 6, 2017

Accepted: June 12, 2017

Published: June 15, 2017

Copyright © 2017 by authors and Scientific Research Publishing Inc. This work is licensed under the Creative Commons Attribution International License (CC BY 4.0).
<http://creativecommons.org/licenses/by/4.0/>



Open Access

Abstract

This paper proposes an extension of the algorithm in [1], as well as utilization of the wavelet transform in event detection, including High Impedance Fault (HIF). Techniques to analyze the abundant data of PMUs quickly and effectively are paramount to increasing response time to events and unstable parameters. With the amount of data PMUs output, unstable parameters, tie line oscillations, and HIFs are often overlooked in the bulk of the data. This paper explores model-free techniques to attain stability information and determine events in real-time. When full system connectivity is unknown, many traditional methods requiring other bus measurements can be impossible or computationally extensive to apply. The traditional method of interest is analyzing the power flow Jacobian for singularities and system weak points, attained by applying singular value decomposition. This paper further develops upon the approach in [1] to expand the Discrete-Time Jacobian Eigenvalue Approximation (DDJEA), giving values to significant off-diagonal terms while establishing a generalized connectivity between correlated buses. Statistical linear models are applied over large data sets to prove significance to each term. Then the off diagonal terms are given time-varying weights to account for changes in topology or sensitivity to events using a reduced system model. The results of this novel method are compared to the present errors of the previous publication in order to quantify the degree of improvement that this novel method imposes. The effective bus eigenvalues are briefly compared to Prony analysis to check similarities. An additional application for biorthogonal wavelets is also introduced to detect event types, including the HIF, for PMU data.

Keywords

Synchrophasor, PMU, openPDC, Power Flow Jacobian, Decoupled Discrete-Time Jacobian Approximation (DDJEA), Singular Value Decomposition (SVD), High Impedance Fault (HIF), Discrete Wavelet Transform (DWT)

1. Introduction

Without system topology, many traditional methods to compute power flow and state estimation cannot be used. One of the more famous industry applications similar to the proposed method is generating the power flow Jacobian used in the Newton-Raphson method. Analyzing the power flow Jacobian as it approaches singularity has been used in [2] [3] [4] to assess system weak points and indicate unstable parameters in the system. The decoupled Jacobian is used in [5] [6] to decrease the necessary number of Newton-Raphson iterations while providing very similar accuracy. These applications are focused on monitoring the eigenvalues of the power flow Jacobian at each bus in order to determine both the unstable condition and system weak points. Due to its computational simplicity, the use in [5] [6] of the decoupled power flow Jacobian showed that only utilizing the partial derivative of real power with respect to bus voltage angle and the partial derivative of reactive power with respect bus voltage magnitude were sufficient for accurate state estimation. Singular Value Decomposition and eigenvalue analyses are powerful tools for monitoring as the Jacobian approaches singularity. Changes in the decoupled power flow Jacobian can occur over time, so it is crucial to distinguish between a slow divergence to a new equilibrium from a slow trend toward instability. Prony Analysis and Frequency Domain Decomposition have been implemented to determine undamped tie line oscillations [7] [8] and inter-area oscillations [9]. It has also been applied to ringdown data [10]. Other methods for identifying power flow modes and eigenvalues are compared with Prony Analysis, including Matrix Pencil Method and Hankel Total Least Squares [11]. These are some of the primary contenders when checking poorly damped power oscillations. Although Prony analysis can be more computationally intensive, [11] shows that it is less effected by noisy measurements. PMU data for large utility systems yields noise due to the variability which simulations often fail to adequately model. This is inherent to the unpredictability of power system operation in real-time. These modes and damping ratios can be used to cross check changes in the Jacobian. When the Jacobian suddenly changes, it can be due to a fault, load switch, capacitor bank, high impedance fault, breaker, or other system operation. Capacitors and large loads can affect a Jacobian temporarily, but those operations are necessary and unless the system parameters are strained, will not result in a major system event. When the Jacobian changes drastically, the most tragic culprits are typically fault or the removal of a necessary line to supply load. The Jacobian can be

used to check the weak buses of the system in real-time and determine the unstable parameter, but a list of recent detected events could easily aid the process in forming a solution. Previously, a discreet time Jacobian eigenvalue approximation was introduced to make use of PMU data without needing system connectivity, and Prony analysis was used to monitor system modes [1].

Detection and identification of event type yields crucial information when determining the current system state. Certain events, primarily the HIF, can be difficult to detect and flag from other system events. Any of the other system events produce more notable transients, but the HIF can stay in a system for a period before suddenly becoming a low impedance fault. This poses a risk to personal safety and grid stability. Ground ratio relays and analysis of harmonic distortion has been used [12] [13]. Time domain solutions like ground ratio relays can be ineffective, particularly in the case of phase imbalance which is more of a problem in distribution. The Kalman filtering approach is used in [13], but there are assumptions that need to be made in order to relate back to the time domain. Frequency domain solutions can often be difficult to relate in real time to the original measurement. Wavelet transforms are applied in [12] [14] [15] [16] [17] to detect HIF cases and distinguish the multilevel characteristics in order to identify events. However, these applications used transient phase current data. This gives point to point resolution that can be a thousand fold faster than PMU data. Wavelets are particularly powerful since the transform can be used to relate frequency data to the time domain. Since HIF data produces time varying frequency distortion, it is difficult to discern the characteristics of the HIF using a time domain or frequency domain approach exclusively [12] [16] [17].

In a system with (N) total buses and (n) buses containing PMUs, utilizing only the subset of the system with PMUs is ideal as a stand-alone process, especially when (n) is much smaller than (N). Industry data from open PDC does not contain connectivity data or Y_{bus} parameters. This renders traditional power flow method utilizing the power flow Jacobian or other methods like Gauss-Seidel unusable. Even with the full system connectivity, if there are 70 buses with PMUs and 3200 buses total in the system, several state estimation iterations are necessary to generate the bus voltages and angles for the remaining buses. The greatest advantage of PMU data is that it can be returned every 60 Hz cycle. Even if the connectivity is available in a system with (N) buses, where the number of PMUs (n) is much smaller, traditional power flow methods are computational expensive and time consuming to apply. In the time it takes to calculate the whole Jacobian for a large system, the speed of the PMU data is likely wasted since only the PMU readings at the beginning of the process would be taken into account. The algorithm needs to converge before the next iteration is read for most effective use of PMU measurements. In a previous publication, PMU data was used from simulation and industry in order to generate an approximation of the eigenvalues for the decoupled power flow Jacobian eigenvalues (DDJEA) at each bus (n). Prony analysis was employed to test the speed and accuracy of the algorithm, as well as help identify system modes. It would be more advantageous

for industry to monitor the subset of the system with PMU data as a standalone process to aid system operators in real time. Certain events like the HIF can be seen in data immediately following an event, most commonly through transient data, but the event has a time varying and non-linear nature and is easily missed in low resolution data or when looking over a large window. It is best to not wait as the HIF becomes a low impedance fault and affects the Jacobian elements significantly. Therefore, industry would benefit by detecting the early signs of a major event rather than waiting for a major event to occur.

This paper proposes a novel method to generate the off-diagonal terms that are most important to each individual bus. This approximate Jacobian only considers buses with PMUs since the overall system model is presumed to be unknown, encompassing all connectivity and load data. In a sense, this creates a reduced connectivity matrix for the system. Linear models are built employed over large data sets in order to determine the significance of each off-diagonal term in the matrix. All insignificant terms are set to zero, implying no reduced connectivity between those particular buses with a PMU installed. This paper will prove that the proposed method functions as a more accurate decoupled Jacobian approximation, and the corresponding eigenvalues of the expanded matrix are more effective in relaying urgency when unstable system parameters develop. The output of Prony analysis is compared in relative speed and accuracy when identifying unstable parameters. The 1-D biorthogonal wavelet transform is utilized on six system values derived from PMU outputs for event detection and identification: real power, reactive power, phase voltage magnitude, phase current magnitude, discrete derivative of current phase angle, and discrete derivative of voltage phase angle. From these characteristics, event location and identification is achieved, including HIF detection. Identifying the cause of power oscillations and changes in the approximated Jacobian can flag undesirable scenarios long before those parameters become unstable.

2. Decoupled Discrete-Time Eigenvalue Approximation Expansion

2.1. Expanding DDJEA to EDDJA for ΔP_i

The next two sections present the derivation of the Expanded Jacobian Approximation Method (EDDJA). In this section, matrices are shown to make the derivation more tangible. In the following section 2.2, several of these matrices will be presented in a more succinct format.

Before proceeding to the derivation, there are several assumptions and justifications presented in [1], a few of which will briefly be addressed. The term " Δt " denotes the time between two PMU measurements. This is synonymous with the sampling frequency, 30 Hz. The smaller the step size, Δt , the more accurately it represents the Jacobian approximation. In [1] it is shown that the Jacobian values should not vary drastically between two measurements unless under a serious system event, in which case the changes in the previous Jacobian approximation and current Jacobian approximation can be compared term by term to

aid in the identification of the event. In context of this paper, $(t + \Delta t)$ should actually denote the most current measurement. Between time steps, the algorithm is validated by applying the changes in bus angle and voltage and then comparing the predicted values to the actual values measured.

The Newton-Raphson approach starts with initial guesses for certain buses, computes an initial guess at the Jacobian, and then iterates updating the real power, reactive power, bus voltage, and bus voltage angle. These values continue to update the Jacobian until the error converges to zero for the power and angle. The advantage of PMU data is that PMUs return the phasor data, which does not need to be updated or changed. If all buses contain a PMU, then the Jacobian can be instantaneously calculated at every time step without any need for further computations. The proposed method accounts for only the buses with a PMU attached. It is important to note that the proposed method provides a similar function but it is not fundamentally the same as the Jacobian since it cannot account for all terms in the full system model. Certain terms in the EDDJA method are affected by buses that are not necessarily known or measured; they are part of the entire system model but not the subset of buses with PMUs installed. By showing that the reduced approximate Jacobian generates an error of approximately zero in the next iteration, the function is shown to be adequate without full system connectivity being necessary.

The formal definition of the decoupled real power portion of the power flow Jacobian is presented in Equation (1). The variable (N) represents the total number of system buses, including those with a PMU connected and those without. The variable (n) is used to notate the total number of buses with installed PMUs.

$$\Delta P_i = \sum_{j=1}^N \frac{\partial P_i}{\partial \delta_j} * \Delta \delta_j. \quad (1)$$

At a particular bus (i), ΔP_i is the change in power at bus (i). This change is calculated by multiplying and summing the difference in all bus angles $\Delta \delta_j$ from the previous measurement by the partial derivative of bus power with respect to each bus angle δ_j . The formal definition of the partial derivative of power at bus (i) with respect to bus (j) angle, δ_j is presented in Equation (2).

$$\frac{\partial P_i}{\partial \delta_j} = -|Y_{ij} V_i V_j| \sin(\theta_{ij} + \delta_j - \delta_k). \quad (2)$$

Y_{ij} represents the p.u. value of the Y_{bus} equivalent admittance between buses (i) and (j), or in the case of (i) and (j) being equivalent, the corresponding diagonal matrix term. When buses are not directly connected, a zero is placed in the matrix for that term. The phase angle relative to Y_{ij} , θ_{ij} is in radians. V_i and V_j are the relative p.u. voltages of the buses (i) and (j) respectively.

The decoupled power flow Jacobian matrix referring to real power is presented in Equation (3) for the application of this paper, where Δt constitutes the time since the last calculation was performed until the newest reading.

$$\begin{bmatrix} \Delta P_1(t + \Delta t) \\ \vdots \\ \Delta P_N(t + \Delta t) \end{bmatrix} = \begin{bmatrix} \frac{\partial P_1}{\partial \delta_1} & \frac{\partial P_1}{\partial \delta_2} & \cdots & \frac{\partial P_1}{\partial \delta_n} \\ \frac{\partial P_2}{\partial \delta_1} & \frac{\partial P_2}{\partial \delta_2} & \cdots & \frac{\partial P_2}{\partial \delta_n} \\ \vdots & \vdots & \ddots & \vdots \\ \frac{\partial P_n}{\partial \delta_1} & \frac{\partial P_n}{\partial \delta_2} & \cdots & \frac{\partial P_n}{\partial \delta_n} \end{bmatrix} \begin{bmatrix} \Delta \delta_1(t + \Delta t) \\ \vdots \\ \Delta \delta_n(t + \Delta t) \end{bmatrix}. \quad (3)$$

In [1], it was shown that a discrete derivative approach was sufficient to ascertain the majority of information available through the buses with PMUs and generate the diagonal terms. This led to an eigenvalue matrix to approximate the Jacobian's eigenvalues presented in Equation (4) for the decoupled real power portion.

$$\begin{bmatrix} \Delta P_1(t + \Delta t) \\ \vdots \\ \Delta P_n(t + \Delta t) \end{bmatrix} = \begin{bmatrix} \frac{\Delta P_1(t)}{\Delta \delta_1(t)} & 0 & 0 \\ 0 & \ddots & 0 \\ 0 & 0 & \frac{\Delta P_n(t)}{\Delta \delta_n(t)} \end{bmatrix} \begin{bmatrix} \Delta \delta_1(t + \Delta t) \\ \vdots \\ \Delta \delta_n(t + \Delta t) \end{bmatrix}. \quad (4)$$

The error associated with the DDJEA method was calculated using Equation (5) and presented in **Table 1**.

$$P_{err} = \frac{P_{actual} - P_{predicted}}{P_{actual}} * 100. \quad (5)$$

$$P_i(t + \Delta t)_{predicted} = P_{iacutal}(t) + \Delta P_i(t + \Delta t). \quad (6)$$

$$P_i(t + \Delta t)_{actual} = 3 * V_{li} * I_{litotal} * \cos(\delta_{V_{li}} - \delta_{I_{li}}). \quad (7)$$

V_{li} is the corresponding average positive sequence voltage magnitude at a bus (i). $I_{litotal}$ is the average net positive sequence current flowing through bus (i). The corresponding phase angle for V_{li} is $\delta_{V_{li}}$, and $\delta_{I_{li}}$ is the phase angle for $I_{litotal}$.

The predicted change calculated via the DDJEA matrix of the previous iteration was compared to the actual value measured during the next iteration. Assuming that the Jacobian should not change dramatically, unless under a serious system event, the assumption was made that the 0.0333 second interval would be sufficiently small enough to apply the Jacobian of the last cycle and compare the

Table 1. DDJEA accuracy for real power estimation.

Calculation source	Percent error of real power (P_{err}) for measurements	
	Mean percent error (P_{err})	Median percent error (P_{err})
IEEE 14 bus simulation	0.054%	$9.51 \times 10^{-6}\%$
Open PDC measurements	0.1977%	0.1003%

changes in the eigenvalue. This theory was shown to hold in [1]. The proposed expansion should ultimately take the form of Equation (8). The expansion of the DDJEA matrix, abbreviated EDDJA for further reference, increases the number of critical terms in the matrix through statistical analysis and least squares analysis. This portion of the expansion is better suited to an offline analysis. Although the process is quick, it would not be applicable for a real-time calculation since a large running window of data is needed first. Once the model is built, it is applicable for constant use in future matrices.

$$\begin{bmatrix} \Delta P_1(t + \Delta t) \\ \vdots \\ \Delta P_n(t + \Delta t) \end{bmatrix} = \begin{bmatrix} \alpha_{11}(t) \frac{\Delta P_1(t)}{\Delta \delta_1(t)} & \alpha_{12}(t) \frac{\Delta P_1(t)}{\Delta \delta_2(t)} & \dots & \alpha_{1n}(t) \frac{\Delta P_1(t)}{\Delta \delta_n(t)} \\ \alpha_{21}(t) \frac{\Delta P_2(t)}{\Delta \delta_1(t)} & \alpha_{22}(t) \frac{\Delta P_2(t)}{\Delta \delta_2(t)} & \dots & \alpha_{2n}(t) \frac{\Delta P_2(t)}{\Delta \delta_n(t)} \\ \vdots & \vdots & \ddots & \vdots \\ \alpha_{n1}(t) \frac{\Delta P_n(t)}{\Delta \delta_1(t)} & \alpha_{n2}(t) \frac{\Delta P_n(t)}{\Delta \delta_2(t)} & \dots & \alpha_{nn}(t) \frac{\Delta P_n(t)}{\Delta \delta_n(t)} \end{bmatrix} \begin{bmatrix} \Delta \delta_1(t + \Delta t) \\ \vdots \\ \Delta \delta_n(t + \Delta t) \end{bmatrix} \quad (8)$$

In order to determine significant terms, a linear model was built over 4000 real power samples per bus from actual industry PMU data. This results in a [4000 × n] matrix that applies least squares analysis to determine significant terms. The Gaussian distribution of each term is used to evaluate the usefulness of the overall model and significance of each individual term. All non-significant terms become 0 while the significant terms will hold a value. The significant terms will not ultimately hold the value assigned by the linear model, since the linear model produces constant terms without a time-varying property. Due to the chaos of this sample, the linear model is ineffective in managing the residual errors, causing a poor value over a long sampling period for the coefficient of determination, R². However, this will be resolved in the following derivations since the linear model assumes a constant value per term instead of the time varying weights desired in Equation (8). For a single bus at time t + Δt, the equation for power would be:

$$\Delta P_i(t + \Delta t) = \sum_{j=1}^n \alpha_{ij}(t) * \frac{\Delta P_i(t)}{\Delta \delta_j(t)} * \Delta \delta_j(t + \Delta t) \quad (9)$$

The term α_{ij}(t) represents the time varying weights. Any terms deemed insignificant will have an α_{ij}(t) term that is permanently set to zero.

From a statistics standpoint, it is initially assumed that each term is important, and may be entirely responsible for the change in power. These terms can be written for each individual bus (i) across all buses (j). Equation (10) shows the individual variables relevant to generating the linear model for bus (i). Equation (10) shows a sample calculation for one term at bus (i). Equation (12) generalizes Equation (11) for the first term of bus 1. Bus 1 is used for the example in Equation (13) and Equation (14).

$$x_i(t + \Delta t) = \sum_{j=1}^n x_{ij}(t + \Delta t) \quad (10)$$

$$x_{i1}(t + \Delta t) = \frac{\Delta P_1(t)}{\Delta \delta_1(t)} * \Delta \delta_1(t + \Delta t) \quad (11)$$

$$x_{11}(t + \Delta t) = \frac{\Delta P_1(t)}{\Delta \delta_1(t)} * \Delta \delta_1(t + \Delta t) \quad (12)$$

Each independent variable takes the form of a column vector. $\Delta P_{1actual}$ is a column vector storing the actual change in power at each time interval. The column vector X_{11} is used to show the predicted value of the change in power at bus (1) by assuming all change is due to the angle of bus (1). It is important to note that for (n) PMU buses, there will be (n) X column vectors for every $\Delta P_{1actual}$ column vector. There are a total of (n) $\Delta P_{1actual}$ column vectors that are used to individually define the outcome for the linear model at each bus (i).

$$X_{11} \text{ (dimension } 4000 \times 1) = \begin{bmatrix} x_{11}(t + \Delta t) \\ x_{11}(t + 2\Delta t) \\ \vdots \\ x_{11}(t + 4000\Delta t) \end{bmatrix} \quad (13)$$

$$\Delta P_{1actual} \text{ (dimension } 4000 \times 1) = \begin{bmatrix} \Delta P_{1actual}(t + \Delta t) \\ \Delta P_{1actual}(t + 2\Delta t) \\ \vdots \\ \Delta P_{1actual}(t + 4000\Delta t) \end{bmatrix} \quad (14)$$

Each bus has (n) X column vectors to be statistically evaluated. The linear model uses least squares to fit a weight to each variable for the overall sample period. If an X value is substituted, the weights will return the overall change in bus power. The final linear model for bus 1 is shown in Equation (15) and expanded generically in Equation (16). R code was used to carry out this analysis.

$$\Delta P_1(T) = \sum_{j=1}^n \beta_{1j} * X_{1j}(T) \quad (15)$$

This equation assumes that the time T is at the exact instance desired. β_{1j} is the weight given to the term correlating the change in real power at bus (1) with respect to bus (j). Unlike equation (6), the weight of each term is not time varying; it is set to a constant by the least squares optimization.

$$\Delta P_1(T) = \beta_{11} * X_{11}(T) + \beta_{12} * X_{12}(T) + \beta_{13} * X_{13}(T) * \dots * \beta_{1n} * X_{1n}(T) \quad (16)$$

The p_{value} of the overall model is then determined to evaluate the significance of the model. All values for $T = t$ to $T = t + 4000\Delta t$ are considered. A p_{value} less than 0.05 generally will suffice to show that the model is significant, but this term can be set to a different value. This would equivalently mean that the model has a 95% chance of being significant. For this particular application, the level of significance was much lower. The overall linear model for the industry system yielded a p_{value} less than 10^{-12} , meaning that the null hypothesis would be rejected: the overall model was significant. In perspective, this means that there is a $10^{-10}\%$ chance that the model is not significant. Then the importance of each

term was tested, setting 0.0001 as the level of significance (a 99.99% threshold that each term considered is significant), in order to determine a single term's effectiveness at predicting the real power change. Only those with lower P_{value} calculations would remain, meaning that individually those terms were adequate to predict the change in real power. This reduction for non-significant terms is shown in Equation (17).

$$\text{For } p_{\beta_{ii}} > 0.0001, \beta_{ii} = 0 \tag{17}$$

All nonzero terms are then placed back in the matrix, and all insignificant terms become zero, showing that there is no connectivity in the reduced model. All off-diagonal terms that are non-zero imply a strong correlation between the buses, and in the context of the power flow Jacobian, some generalization of connectivity. However, the weights used for the overall model are not adequate when looking at longer time periods. In order to get a running window, an overdetermined equation is formed in order to solve for the weights of all non-zero terms in real-time. The mathematical concept is demonstrated with a 4 bus model for simplicity. In this model, there is connectivity between buses 1 and 2, as well as 3 and 4.

$$\begin{bmatrix} \Delta P_1(t + \Delta t) \\ \Delta P_2(t + \Delta t) \\ \Delta P_3(t + \Delta t) \\ \Delta P_4(t + \Delta t) \end{bmatrix} = \begin{bmatrix} \alpha_{11}(t) \frac{\Delta P_1(t)}{\Delta \delta_1(t)} & \alpha_{12}(t) \frac{\Delta P_1(t)}{\Delta \delta_2(t)} & 0 & 0 \\ \alpha_{21}(t) \frac{\Delta P_2(t)}{\Delta \delta_1(t)} & \alpha_{22}(t) \frac{\Delta P_2(t)}{\Delta \delta_2(t)} & 0 & 0 \\ 0 & 0 & \alpha_{33}(t) \frac{\Delta P_3(t)}{\Delta \delta_3(t)} & \alpha_{34}(t) \frac{\Delta P_3(t)}{\Delta \delta_4(t)} \\ 0 & 0 & \alpha_{43}(t) \frac{\Delta P_4(t)}{\Delta \delta_3(t)} & \alpha_{44}(t) \frac{\Delta P_4(t)}{\Delta \delta_4(t)} \end{bmatrix} \begin{bmatrix} \Delta \delta_1(t + \Delta t) \\ \Delta \delta_2(t + \Delta t) \\ \Delta \delta_3(t + \Delta t) \\ \Delta \delta_4(t + \Delta t) \end{bmatrix} \tag{18}$$

In order to calculate the variable terms in a single row, the equation can be set up ignoring all zero terms. If the number of non-zero terms is M , in this case $M = 2$ for each row, then a running window of $M + 1$ equations is necessary to apply least squares. The back calculation for α_{11} and α_{12} are as follows in Equations (19 - 22).

$$\begin{bmatrix} \Delta P_1(t - 2\Delta t) \\ \Delta P_1(t - \Delta t) \\ \Delta P_1(t) \end{bmatrix} = \begin{bmatrix} x_{11}(t - 2\Delta t) & x_{12}(t - 2\Delta t) \\ x_{11}(t - \Delta t) & x_{12}(t - \Delta t) \\ x_{11}(t) & x_{12}(t) \end{bmatrix} \begin{bmatrix} \alpha_{11}(t) \\ \alpha_{12}(t) \end{bmatrix} \tag{19}$$

$$A = \begin{bmatrix} x_{11}(t - 2\Delta t) & x_{12}(t - 2\Delta t) \\ x_{11}(t - \Delta t) & x_{12}(t - \Delta t) \\ x_{11}(t) & x_{12}(t) \end{bmatrix} \tag{20}$$

$$B = \begin{bmatrix} \Delta P_1(t - 2\Delta t) \\ \Delta P_1(t - \Delta t) \\ \Delta P_1(t) \end{bmatrix} \quad (21)$$

$$\begin{bmatrix} \alpha_{11}(t) \\ \alpha_{12}(t) \end{bmatrix} = (A^T A)^{-1} * A^T * B \quad (22)$$

In an extensive system, it is worthwhile to run a sufficiently large sample size offline to attain a generalized system topology between the PMU buses. Then that topology can be used for online application. Before the running window has been met, $M + 1$ full readings, the original DDJEA method is implemented, using the eigenvalue approximation approach to estimate critical system information. Once the necessary window has been met, the EDDJA method is applied to calculate weights for each component. Unlike the linear model constants, these weights change with time. Each weight is calculated over a very small time period, since the Jacobian should not change significantly. These weights allow the impact and importance of each term to change over time, especially as system conditions change or during an event such as a fault. The R^2 value of the individual models tend to be above 0.9995 with almost all error reduced from each windowed model, effectively solving the main concern of using a universal variable to calculate the weight of each term. The general connectivity is solved over one long running window, but the individual terms can take different magnitudes and sign over days.

Equation (5) is applied to the outcome of using the DDJEA method from Equation (4) in order to estimate the power at the $t + \Delta t$ time step for **Table 1**. Equation (5) is also used to calculate the percent error when using the expanded discreet Jacobian approximation, EDDJA, in Equation (8) to ascertain the effectiveness of the EDDJA method. The percent error of the predicted real power and actual real power is improved by the EDDJA method for both simulated and real industry case, with the DDJEA and EDDJA methods displayed in **Table 1** and **Table 2**. The industry system had the outputs recorded for 147.5 seconds, 4225 individual time steps, same as in [1] for comparison of the methods. The IEEE 14 bus system was simulated with a three phase fault which cleared via line removal after 0.1 seconds. **Table 3** shows the magnitude of error that was reduced by using EDDJA over DDJEA to approximate the next real power state.

By increasing the number of important terms and giving those terms weights based on a running least square windowing method, EDDJA reduces the percent error by orders of magnitude shown in **Table 3**.

The reduction of error in both the simulated and real industry systems was similar, with the method being even more effective in reducing error for the real system. Due to the complexity and unpredictability of the actual system, it is reasonable to notice that there is inherently more error in the predicted power values. However, the mean percent error of both systems is noticeably similar. The median percent error of both cases in drastically reduced as well. The simulation shows a median percent error that is effectively zero, but this is due to the

Table 2. EDDJA accuracy for real power estimation.

calculation source	Percent Error of real power (P_{err}) for measurements	
	Mean percent error (P_{err})	Median percent error (P_{err})
IEEE 14 bus Simulation	0.0012%	$1.25 \times 10^{-7}\%$
Open PDC measurements	0.0034%	0.0013%

Table 3. EDDJA error reduction compared to DDJEA.

Calculation source	Percent error reduction of real power (P_{err}) measurements	
	Mean percent error magnitude reduction	Median percent error magnitude reduction
IEEE 14 bus simulation	45x	76x
Open PDC measurements	58x	77x

linearity and reduced complexity of a simulated system. EDDJA produced an approximate Jacobian than adequately fulfilled the function of the actual decoupled power flow Jacobian. It also out-performed the DDJEA method previously introduced.

2.2. Expanding DDJEA to EDDJA for ΔQ_i

The derivation for the decoupled reactive power portion of the Jacobian follows the same pattern as the real power portion of the decoupled Jacobian. The following equations present the derivations for ΔQ_b , the change in reactive power at bus (i). All mathematical notation follows the same notation as the equations in section 2.1.

$$\Delta Q_i = \sum_{j=1}^N |V_i| * \frac{\partial Q_i}{\partial |V_j|} * \left| \frac{\Delta V_j}{V_j} \right|. \tag{23}$$

$$\frac{|V_i| \partial Q_i}{\partial |V_j|} = -|V_i| |Y_{ij} V_i V_j| \sin(\theta_{ij} + \delta_j - \delta_k). \tag{24}$$

$$\therefore Q_i(t + \Delta t)_{predicted} = Q_i(t) + \Delta Q_i(t + \Delta t) \tag{25}$$

$$Q_i(t + \Delta t)_{actual} = 3 * V_{li} * I_{ltotal} * \sin(\delta_{Vli} - \delta_{li}). \tag{26}$$

$$\begin{bmatrix} \Delta Q_1(t + \Delta t) \\ \vdots \\ \Delta Q_n(t + \Delta t) \end{bmatrix} = \begin{bmatrix} \frac{\Delta Q_1(t)}{|\Delta V_1(t)|} * |V_1(t)| & 0 & 0 \\ 0 & \ddots & 0 \\ 0 & 0 & \frac{\Delta Q_n(t)}{|\Delta V_n(t)|} * |V_n(t)| \end{bmatrix} \begin{bmatrix} \left| \frac{\Delta V_1(t + \Delta t)}{V_1(t + \Delta t)} \right| \\ \vdots \\ \left| \frac{\Delta V_n(t + \Delta t)}{V_n(t + \Delta t)} \right| \end{bmatrix}. \tag{27}$$

$$Q_{err} = \frac{Q_{actual} - Q_{predicted}}{Q_{actual}} * 100. \tag{28}$$

$$\begin{bmatrix} \Delta Q_1(t + \Delta t) \\ \vdots \\ \Delta Q_N(t + \Delta t) \end{bmatrix} = \begin{bmatrix} \frac{\partial Q_1}{\partial |V_1|} * V_1 & \frac{\partial Q_1}{\partial |V_2|} * V_1 & \dots & \frac{\partial Q_1}{\partial V_n} * V_1 \\ \frac{\partial Q_2}{\partial V_1} * V_2 & \frac{\partial P_2}{\partial V_2} * V_2 & \dots & \frac{\partial P_2}{\partial \delta_n} * V_2 \\ \vdots & \vdots & \ddots & \vdots \\ \frac{\partial P_n}{\partial \delta_1} * V_n & \frac{\partial P_n}{\partial \delta_2} * V_n & \dots & \frac{\partial P_n}{\partial \delta_n} * V_n \end{bmatrix} \begin{bmatrix} \frac{\Delta V_1(t + \Delta t)}{V_1(t + \Delta t)} \\ \vdots \\ \frac{\Delta V_n(t + \Delta t)}{V_n(t + \Delta t)} \end{bmatrix}. \tag{29}$$

$$\begin{bmatrix} \Delta Q_1(t + \Delta t) \\ \vdots \\ \Delta Q_n(t + \Delta t) \end{bmatrix} = \begin{bmatrix} \alpha_{11}(t) \frac{\Delta Q_1(t)}{\Delta V_1(t)} * V_1(t) & \alpha_{12}(t) \frac{\Delta Q_1(t)}{\Delta V_2(t)} * V_1(t) & \dots & \alpha_{1n}(t) \frac{\Delta Q_1(t)}{\Delta V_n(t)} * V_1(t) \\ \alpha_{21}(t) \frac{\Delta Q_2(t)}{\Delta V_1(t)} * V_2(t) & \alpha_{22}(t) \frac{\Delta Q_2(t)}{\Delta V_2(t)} * V_2(t) & \dots & \alpha_{2n}(t) \frac{\Delta Q_2(t)}{\Delta V_n(t)} * V_2(t) \\ \vdots & \vdots & \ddots & \vdots \\ \alpha_{n1}(t) \frac{\Delta Q_n(t)}{\Delta V_1(t)} * V_n(t) & \alpha_{n2}(t) \frac{\Delta Q_n(t)}{\Delta V_2(t)} * V_n(t) & \dots & \alpha_{nm}(t) \frac{\Delta Q_n(t)}{\Delta V_n(t)} * V_n(t) \end{bmatrix} \begin{bmatrix} \frac{\Delta V_1(t + \Delta t)}{V_1(t + \Delta t)} \\ \vdots \\ \frac{\Delta V_n(t + \Delta t)}{V_n(t + \Delta t)} \end{bmatrix}. \tag{30}$$

$$x_{11Q}(t + \Delta t) = \frac{\Delta Q_1(t)}{\Delta V_1(t)} * V_1(t) * \frac{\Delta V_1(t + \Delta t)}{V_1(t + \Delta t)} \tag{31}$$

$$\Delta Q_1(T) = \sum_{j=1}^n \beta_{1j} * X_{1jQ}(T) \tag{32}$$

$$\text{For } p_{\beta_{1i}} > 0.0001, \beta_{1i} = 0 \tag{33}$$

The same IEEE 14 bus system data and industry PMU data were used to test the reactive power case. **Table 4** displays the accuracy of the DDJEA method, while **Table 5** shows the accuracy in predicting the next reactive power state when using the EDDJA algorithm. **Table 6** demonstrates the magnitude of the error reduction by using EDDJA compared to DDJEA.

In the IEEE 14 bus simulation, the error when predicting the reactive power state was reduced almost entirely. For the industry measurements, the errors were reduced significantly, but not by the same margin. Generators are set to supply consistent real power output. The reactive power fluctuates to maintain the real power output. In the simulated system, there was far less variation, even with simulated system events. In the real system, the reactive power fluctuated wildly, something to expect with significantly more loads and 3000 more buses

Table 4. DDJEA accuracy for reactive power estimation.

Calculation source	Percent error of predicted and actual reactive power state (Q_{err})	
	Mean percent error	Median percent error
IEEE 14 bus simulation	0.1884%	$9.104 \times 10^{-7}\%$
Open PDC measurements	0.8916%	0.3342%

Table 5. EDDJA accuracy for reactive power estimation.

Calculation source	Percent error of predicted and actual reactive power state (Q_{err})	
	Mean percent error	Median percent error
IEEE 14 bus simulation	$3.91 \times 10^{-5}\%$	$1.137 \times 10^{-11}\%$
Open PDC measurements	0.1435%	0.1027%

Table 6. EDDJA error reduction compared to DDJEA for reactive power.

Calculation source	Percent error reduction of real power (P_{err}) measurements	
	Mean percent error magnitude reduction	Median percent error magnitude reduction
IEEE 14 bus simulation	4818x	80,070x
Open PDC measurements	6.21x	3.25x

in the overall system. The EDDJA method was able to reduce a significant amount of error from the system while adding a negligible amount to the overall computation time, as much as 40%, converging before the next iteration is read. The EDDJA method generates a reduced matrix that accurately functions as a Jacobian approximation. The novel method also proves itself an improvement in comparison to the DDJEA method for approximating the reactive portion of the decoupled power flow Jacobian.

3. Implementing EDDJA for Situational Awareness and Stability Analysis

When analyzing the decoupled power flow Jacobian, eigenvalue analysis or SVD can be applied to assess system weak points and group buses in terms of sensitivity to an event. For the DDJEA algorithm, the diagonal terms were already the eigenvalues of each particular bus with respect to real and reactive power. When a value near singularity occurs, generally in the case of a fault or line removal, the affected buses can be flagged. Once singularity occurs, the system is already unstable, so developing tools to predict when the eigenvalues are approaching singularity before it occurs are necessary. Also, the eigenvalue bounds of normal system operation need to be determined in order to avoid flagging regular system activity as deviation from the equilibrium points. In a real system and simulated system, the value will rarely converge to a single value. Instead the eigenvalues of each term fluctuate within different acceptable system bounds. Mathematical representations to determine when the DDJEA matrix is accelerating/decelerating and increasing/decreasing are useful when determining whether the eigenvalues are converging or diverging from an equilibrium point. Equations (34 - 36) are applied to the DDJEA method for determining acceleration

and magnitude variation.

EDDJJA requires eigenvalue calculation and Singular Value Decomposition is used to quantify bus eigenvalues into different zones during an event or unstable oscillation. Knowing which buses and parameters are most effected during the onset of unstable conditions can aid system operators in isolating and fixing the issue. The eigenvalue for EDDJJA is similarly utilized in Equations (37 - 39). “ AI ” denotes the acceleration indicator. These equations below are derived for the real power portion of DDJEA and EDDJJA. The reactive power decoupled portions are derived similarly.

$$AI_{DDJEA}(t) = \Delta \left(\frac{\Delta P_i(t)}{\Delta \delta_i(t)} \right) = \left| \left(\frac{\Delta P_i(t)}{\Delta \delta_i(t)} - \frac{\Delta P_i(t-\Delta t)}{\Delta \delta_i(t-\Delta t)} \right) \right| - \left| \left(\frac{\Delta P_i(t-\Delta t)}{\Delta \delta_i(t-\Delta t)} - \frac{\Delta P_i(t-2\Delta t)}{\Delta \delta_i(t-2\Delta t)} \right) \right| \quad (34)$$

$$|AI_{DDJEA}(t)| - |AI_{DDJEA}(t-\Delta t)| > 0 \xrightarrow{\text{yields}} \text{bus DDJEA is accelerating.} \quad (35)$$

$$\left(\left| \frac{\Delta P_i(t)}{\Delta \delta_i(t)} \right| - \left| \frac{\Delta P_i(t-\Delta t)}{\Delta \delta_i(t-\Delta t)} \right| \right) > 0 \xrightarrow{\text{yields}} \text{bus DDJEA is increasing.} \quad (36)$$

$$\left| \left(eig(Bus(i))(t) - eig(Bus(i))(t-\Delta t) \right) \right| - \left| \left(eig(Bus(i))(t-\Delta t) - eig(Bus(i))(t-2\Delta t) \right) \right| \quad (37)$$

$$|AI_{EDDJJA}(t)| - |AI_{EDDJJA}(t-\Delta t)| > 0 \xrightarrow{\text{yields}} \text{bus EDDJJA is accelerating.} \quad (38)$$

$$\left(\left| eig(Bus(i))(t) \right| - \left| eig(Bus(i))(t-\Delta t) \right| \right) > 0 \xrightarrow{\text{yields}} \text{bus EDDJJA is increasing.} \quad (39)$$

Since singularities are the mathematical indication of instability in terms of DDJEA and EDDJJA elements, acceleration toward zero and infinity should always be flagged. By analyzing EDDJJA, both static and dynamic stability margins can be assessed. Furthermore, a continually increasing eigenvalue outside of equilibrium can be flagged so that slow inter-area oscillations are not missed. Immediately after system events, acceleration back toward the equilibrium point is noted and system parameters are updated should a solution not be necessary. In [1], the DDJEA algorithm was applied for situational awareness and flagging critically unstable parameters. Singular Value Decomposition is applied in this model to achieve an index for eigenvalues, similar to [2] [3] [4] [5] [6]. **Figure 1** shows the general algorithm that EDDJJA implements to enhance situational awareness. **Table 7** decodes the output of the graphs for both DDJEA and EDDJJA in **Figure 2** and **Figure 3** respectively. These methods are compared to the output of Prony Analysis in **Figure 4** to showcase EDDJJA’s immediate detection of an unstable system mode in comparison with a well-known method.

The method returns the location of an event or critically unstable eigenvalue, the properties of that eigenvalue in relation to static or dynamic instability dependent upon which portions of the EDDJJA matrix are affected, all other buses and parameters are contributing to the unstable conditions, and a rating of system weak points to the event. **Figure 2** and **Figure 3** show the output for stability margins in reference to the PMU 4, the system’s weak point for this event.

Table 7. DDJEA and EDDJA analysis code value interpretation.

Figure 2/Figure 3 decode table	
code value	Interpretation of Value
0	System is at equilibrium range/No action necessary
5	Bus eigenvalue is converging to a new equilibrium point/No action necessary
10	Slightly divergent trends detected in eigenvalue/No action unless this pattern continues
15	Eigenvalue is converging from unstable parameters/No action unless divergence occurs or after event
20	Bus eigenvalue is marginally converging from unstable parameters/FLAG
25	Eigenvalue at bus is increasing toward dynamic instability/FLAG CRITICAL
30	Eigenvalue is accelerating toward dynamic instability/FLAG CRITICAL
35	Dynamic and voltage instability parameters detected/FLAG CRITICAL
40	Approaching singularity/System will go unstable soon without solution/FLAG CRITICAL
50	Major system event or eigenvalue in range of singularity/FLAG HIGHEST PRIORITY

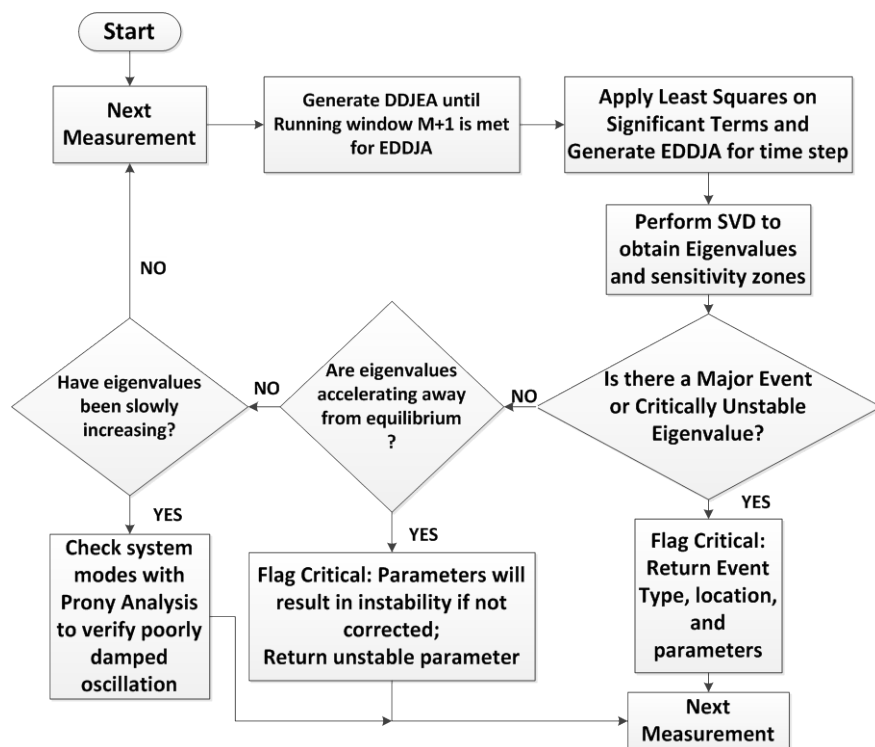


Figure 1. EDDJA analysis for applied situational awareness.

The fault occurs at measurement 1500, and both DDJEA and EDDJA recognize the major system event within 1 cycle. DDJEA is limited to generating only the diagonal approximations, so the eigenvalue calculated appears to converge for short periods of time, but then the system immediately shows divergent, accelerating trends and the indications for both dynamic and static instability: seen

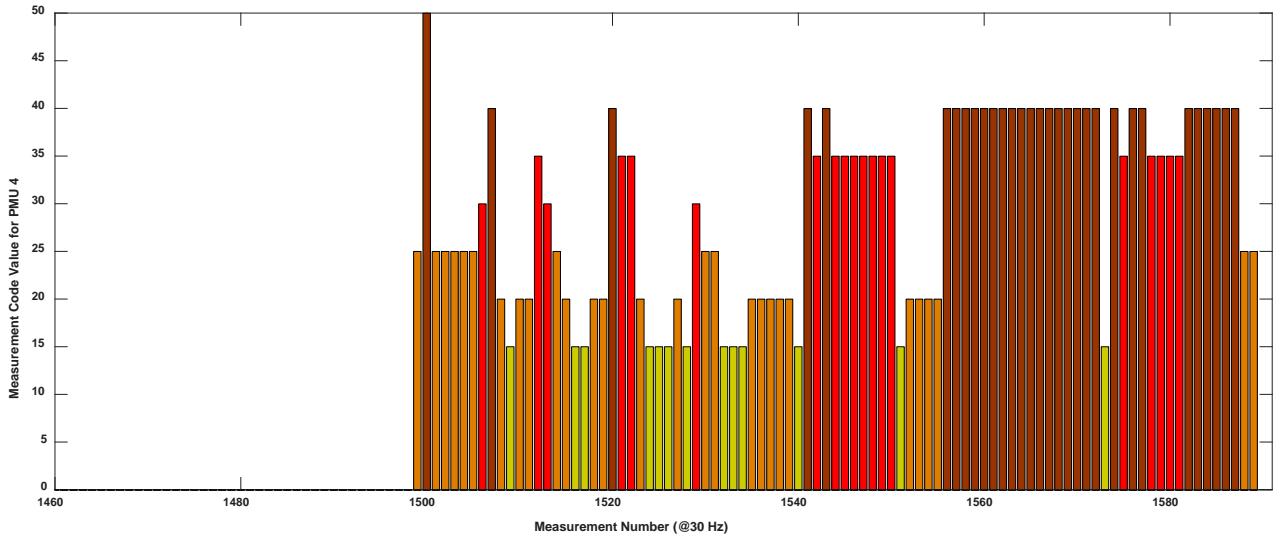


Figure 2. DDJEA analysis output for unstable case.

in **Figure 3**. **Figure 4** demonstrates that the weighted off-diagonal terms are consistently unstable when their time-varying weights are applied. The initial event detection of DDJEA and EDDJA are comparable, but the eigenvalues of the EDDJA matrix show more consistency when identifying both dynamic and static instability due to the additional weighted terms in both the real and reactive power decoupled Jacobian matrix approximations. This implementation of SVD and eigenvalue analysis correlates with [2] [3] [4] [5] [6]. Since the weak point and parameters could have been relayed, this unstable condition could have been prevented by having system operators manually remove the affected line without voltage collapse.

The output of these methods can be compared with event detection using Prony analysis for comparison of effectiveness and response time. It is viable to note that Prony Analysis does not converge in real-time for all buses and therefore is better used to monitor inter-area oscillations, and modes approaching marginally stable conditions [7] [8]. Equations (40) and (41) show the general output of Prony Analysis.

$$F(t) = \sum_{j=1}^M \alpha_j * e^{\sigma_j t} \times \cos(2\pi f_j t + \phi_j). \quad (40)$$

$$F(t) = \sum_{i=1}^M \beta_i e^{\pm j\phi_i} e^{\lambda_i t}. \quad (41)$$

The signal is decomposed into a series of weighted, damped sinusoids. The eigenvalues are put into state-space form, terms with weights near zero are removed, and the fundamental mode and corresponding eigenvalues are returned. The signal under analysis is the real power at each PMU bus. The power through the bus is analyzed for poorly damped or unstable dominant modes. Prony Analysis was applied to the same unstable data set as DDJEA and EDDJA. The interpreted output is shown in **Figure 4** with **Table 8** detailing the individual output levels.

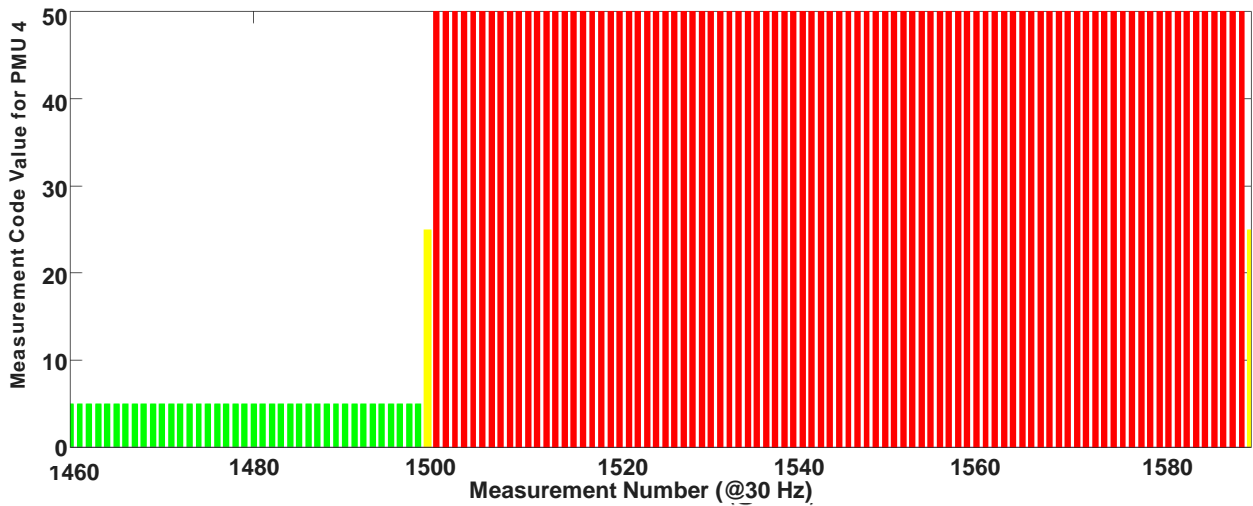


Figure 3. EDDJA analysis output for unstable case.

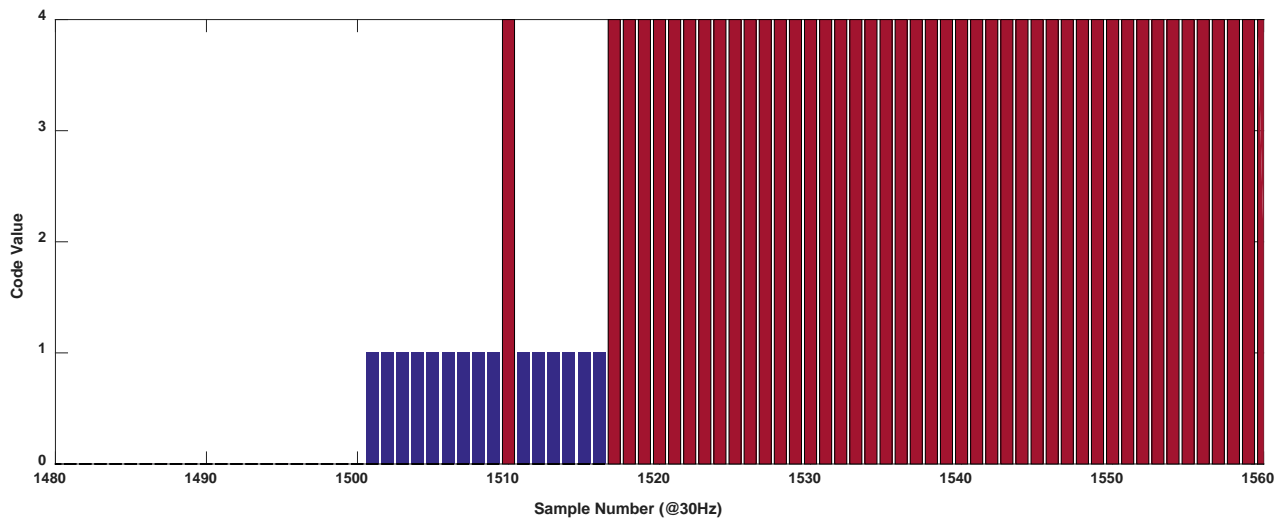


Figure 4. Prony analysis output for unstable case.

Table 8. Prony analysis code value interpretation.

Figure 4 decode table	
Code value	Interpretation of value
0	Damping ratio is above 5% and frequency is not shifting significantly
1	System mode and eigenvalue are shifting significantly
2	Damping ratio under 5%/Flag oscillation
3	Damping ratio is under 1% and eigenvalue's real part is reaching 0/Flag critical
4	A dominant system mode has a positive real part [Unstable condition]/FLAG HIGHEST PRIORITY

Prony analysis detects a significant shift in the dominant mode, but the first unstable eigenvalue is not read for 10 cycles. Prony analysis registers a consistently unstable dominant eigenvalue at the same PMU however after several

cycles have passed, verifying that the EDDJA method more accurately reflects the nature of the bus eigenvalues than the DDJEA method. In terms of situational awareness, Prony analysis is well suited to be run alongside the EDDJA method to help identify and verify unstable power oscillations early on for buses that have marginally divergent EDDJA indications.

4. 1-D Biorthogonal Wavelet Event Detection and Identification

The 1-D discrete biorthogonal wavelet was selected for processing the individual signals. The signals were analyzed with a variety of wavelets including Haar, Meyer, and Symlet wavelets. The Matlab “bior3.5” wavelet function was ultimately used to generate the wavelet coefficients. These coefficients were analyzed across several different cases containing a fault, capacitor switch, HIF, load switch, and line removal. Peak wavelet coefficients for the real power, reactive power, phase voltage magnitude, phase current magnitude, discrete derivative of the voltage phase angle, and discrete derivative of the current phase angle. Equation (42) shows the general format from which the wavelet coefficients are ultimately derived.

$$W_{\psi}(a, d) = \int_{-\infty}^{\infty} x(t) \psi_{a,d}(t) dt \quad (42)$$

$\psi(t)$ is the mother wavelet function, with $\psi_{a,d}$ being made up of orthonormal basis vectors to decompose $x(t)$, the target signal or function. The scope of this paper’s particular application focuses solely on the high frequency wavelet coefficients and a 1-level decomposition for mathematical simplicity and speed during events for convergence. The wavelet transform finds favor in [12] [14] [15] [16] [17] due to the ability to relate changes in the frequency domain back to the time domain. Since HIF frequency distortion is nonlinear and time varying, it is often lost in Fourier transforms and other frequency approaches. Since an HIF insignificantly changes the magnitude of current and voltage, less than the average load, a method that combines time domain and frequency domain approaches was ideal. During an event, the peak amplitude of the wavelet coefficients is recorded for each variable along a running window. Since magnitudes can change based on p.u. ratings and window length, most of the variables will be defined symbolically, although statistical analysis to determine rates of false positives are definitely something to consider when analyzing the system for cutoff variables. Below are some terms that are necessary to explain this method’s approach in Figure 5. Depending on window size and system ratings, these coefficients would need to be run for several test cases. Other variables can be manipulated to fit within a range. Gaussian distributions analyze the odds of a false-positive. Particular ratios are extraordinarily effective when identifying events. All of these wavelets were calculated with the biorthogonal “bior3.5” discrete wavelet transform. As long as the peak wavelet coefficient for real power stays below a threshold, no further analysis is required. A moving window takes into account the newest measurement and analyzes the event until a new peak value is reached.

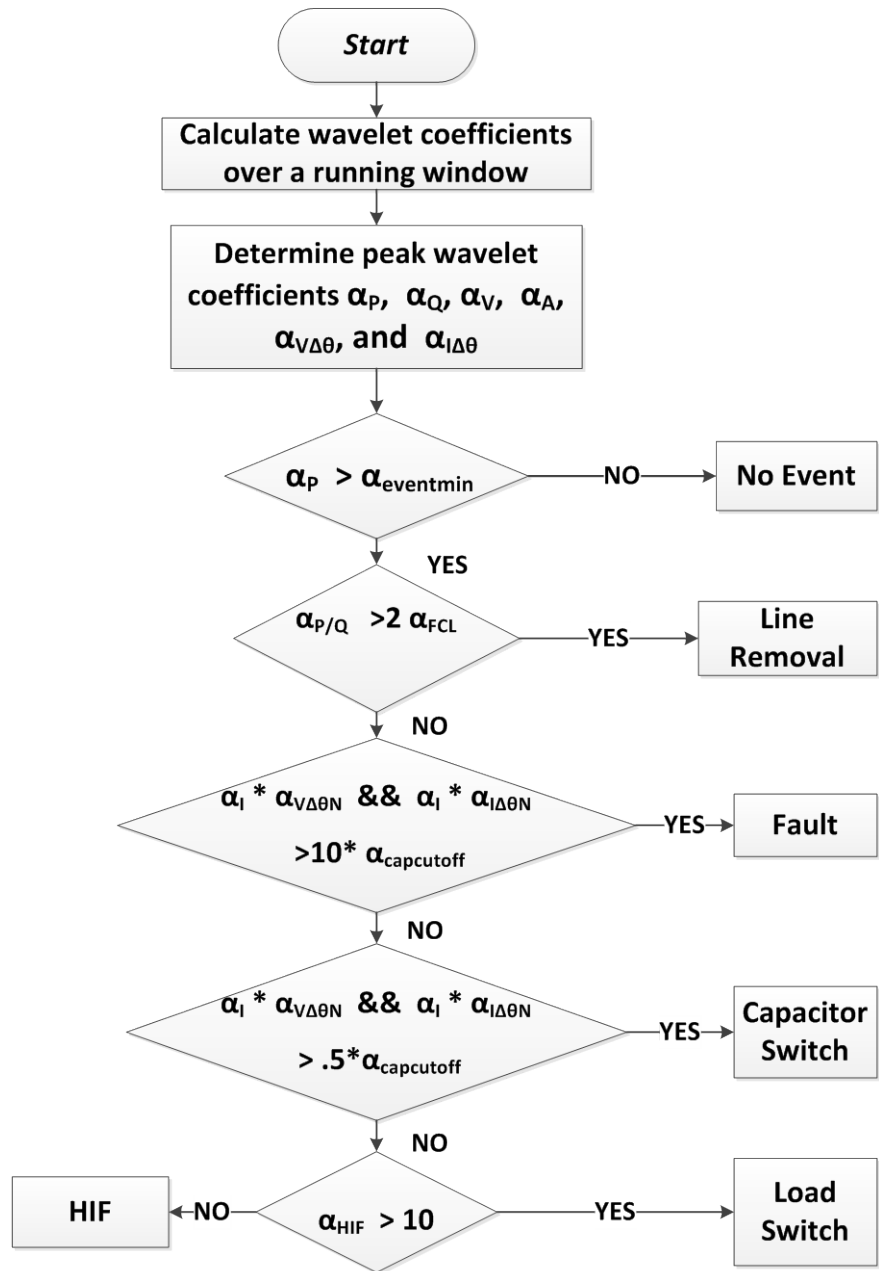


Figure 5. Biorthogonal wavelet event identification.

- α_P → The peak wavelet coefficient associated with the real power signal;
- α_Q → The peak wavelet coefficient associated with the reactive power signal;
- α_V → The peak wavelet coefficient associated with the voltage magnitude signal;
- α_I → The peak wavelet coefficient associated with the current magnitude signal;
- $\alpha_{V\Delta\theta}$ → The peak wavelet coefficient associated with the discrete derivative of current phase angle;
- $\alpha_{I\Delta\theta}$ → The peak wavelet coefficient associated with the discrete derivative of voltage phase angle;

$\alpha_{eventmin}$ → The real power wavelet coefficient used as a cut off many orders above system noise;

$\alpha_{capcutoff}$ → Lower wavelet bound for typical system capacitors in regards to α_P ;

$$\alpha_{P/Q} = \frac{\alpha_P}{\alpha_Q} \quad (43)$$

$\alpha_{P/Q}$ → Gives a margin to easily detect line removals; All other events fall near 1 or under;

α_{FCL} → Calculated by creating a gaussian distribution over a range of data:

→ Then the value is calculated for having a 1% level of significance, meaning that;

→ 1 out of every 100 rejections will be false. When the number is doubled, the odds converge;

→ Toward zero.

$\alpha_{V\Delta\Theta N} = \frac{\alpha_{V\Delta\Theta}}{0.001}$ → This is just an applied weight for certain calculations (44).

$$\alpha_{I\Delta\Theta N} = \frac{\alpha_{I\Delta\Theta}}{0.001} \quad (45)$$

The low impedance fault stands out statistically in wavelet transforms. The HIF can be hard to determine, but it affects the discrete derivative of the voltage angle significantly more in most cases than a load switch. A load switch dwarfs the impact that an HIF appears to have on the system from time domain samples, but by highlighting the one area that HIF has a greater magnitude, a term can be generated that drives a load switch toward a higher value and an HIF toward zero. This guarantees that even a small load switch cannot drive toward zero due to its effect on the circuit. This term is called α_{HIF} .

$$\alpha_{HIF} = \frac{\alpha_{V\Delta\Theta}}{\alpha_{I\Delta\Theta}} \quad (46)$$

Figure 5 shows the general algorithm for applying wavelet transforms for event detection and identification.

In the case of all tested events, this model was able to adequately identify the event type. Statistical analysis is a powerful addition to this model when selected the cutoff values. Analyzing the mean and standard deviation of different event types can help distinguish event characteristics. The detection of HIF characteristics through PMU data was a fantastic breakthrough, since a lot of publications use transient data for detection. PMU data can cover a much larger time segment in fewer points, but there is also less resolution than samples with 1,000,000 Hz sampling rates. This is an advantage since smaller window lengths are required to enclose the event and its residual effects to the system.

5. Conclusion

The proposed novel method excelled in both event detection and reducing error from the predicted state value. The accuracy of EDDJA shows clearly that it can uphold a similar function to the full Jacobian model, especially in a situation

where system connectivity is unavailable, making it an excellent model-free analysis method. The conditions and options to include both Prony analysis and wavelet decomposition were expressed. EDDJA yields incredibly accurate eigenvalue information, leading to more accurate identification of unstable parameters and increased system visibility with respect to which buses are influencing an unstable parameter. Prony analysis verified the estimate of unstable eigenvalues by EDDJA. Prony analysis and wavelet decomposition are both ideal tools to use along with this method to give system operators verification and time to solve oscillatory power flow and event types. In the case of events, wavelet analysis can be used to double check the cause of changes in the Jacobian. The wavelet transform was able to detect and identify all system events including the HIF from PMU data, which is significant since the majority of publications apply wavelet transforms to transient data sets. Future research will most likely incorporate Machine Learning to wavelet outputs to train a more flexible algorithm that can immediately analyze data without further offline analysis.

Acknowledgements

The authors would like to thank the members of Clemson University Electric Power Research Association (CUEPRA) for their financial support and providing PMU data.

References

- [1] Kantra, S.D. and Makram, E.B. (2016) Development of the Decoupled Discrete-Time Jacobian Eigenvalue Approximation for Situational Awareness Utilizing open PDC. *Journal of Power and Energy Engineering*, **4**, 21-35.
<https://doi.org/10.4236/jpee.2016.49003>
- [2] Sauer, P.W. and Pai, M.A. (1990) Power System Steady-State Stability and the Load-Flow Jacobian. *IEEE Transactions on Power Systems*, **5**, 1374-1383.
<http://ieeexplore.ieee.org/stamp/stamp.jsp?tp=&arnumber=99389>
<https://doi.org/10.1109/59.99389>
- [3] Bompard, E., Carpaneto, E., Chicco, G. and Napoli, R. (1996) A Dynamic Interpretation of the Load-Flow Jacobian Singularity for Voltage Stability Analysis. *International Journal of Electrical Power & Energy Systems*, **18**, 385-395.
http://ac.els-cdn.com/0142061595000828/1-s2.0-0142061595000828-main.pdf?_tid=88f8aee4-55d5-11e6-9b87-00000aacb361&acdnat=1469828809_a3d7830991205892bc2111fd63d57c2d
[https://doi.org/10.1016/0142-0615\(95\)00082-8](https://doi.org/10.1016/0142-0615(95)00082-8)
- [4] Lof, P.-A., Smed, T., Andersson, G. and Hill, D.J. (1992) Fast Calculation of a Voltage Stability Index. *IEEE Transactions on Power Systems*, **7**, 54-64.
<http://ieeexplore.ieee.org/stamp/stamp.jsp?tp=&arnumber=141687>
<https://doi.org/10.1109/59.141687>
- [5] Stott, B. and Alsac, O. (1974) Fast Decoupled Load Flow. *IEEE Transactions on Power Apparatus and Systems*, **PAS-93**, 859-869.
<http://ieeexplore.ieee.org/stamp/stamp.jsp?tp=&arnumber=4075431>
<https://doi.org/10.1109/TPAS.1974.293985>
- [6] van Amerongen, R.A.M. (1989) A General-Purpose Version of the Fast Decoupled Load Flow. *IEEE Transactions on Power Systems*, **4**, 760-770.

- <http://ieeexplore.ieee.org/stamp/stamp.jsp?tp=&arnumber=193851>
<https://doi.org/10.1109/59.193851>
- [7] Guoping, L., Ning, J., Tashman, Z., Venkatasubramanian, M. and Trachian, P. (2012) Oscillation Monitoring System Using Synchrophasors. 2012 *IEEE Power and Energy Society General Meeting*, San Diego, CA, 22-26 July 2012, 1-8. <http://ieeexplore.ieee.org/stamp/stamp.jsp?tp=&arnumber=6345444>
<https://doi.org/10.1109/PESGM.2012.6345444>
- [8] Guoping, L. and Venkatasubramanian, M. (2008) Oscillation Monitoring from Ambient PMU Measurements by Frequency Domain Decomposition. 2008 *IEEE International Symposium on Circuits and Systems*, Seattle, WA, 18-21 May 2008, 2821-2824. <http://ieeexplore.ieee.org/xpl/articleDetails.jsp?arnumber=4542044>
<https://doi.org/10.1109/iscas.2008.4542044>
- [9] Bruelmann, H., Grebe, E. and Losing, M. (2000) Analysis and Damping of Inter-Area Oscillations in the UCTE/CENTRAL Power System. <http://citeseerx.ist.psu.edu/viewdoc/download;jsessionid=4C196EE579817D7A450EAA3A662DA104?doi=10.1.1.124.7846&rep=rep1&type=pdf>
- [10] Ning, Z., Huang, Z., Tuffner, S., Pierre, J. and Jin, S. (2010) Automatic Implementation of Prony Analysis for Electromechanical Mode Identification from Phasor Measurements. 2010 *IEEE Power and Energy Society General Meeting*, Minneapolis, MN, 25-29 July 2010, 1-8. <https://doi.org/10.1109/PES.2010.5590169>
http://ieeexplore.ieee.org/xpls/abs_all.jsp?arnumber=5590169&tag=1
- [11] Guoping, L., Quintero, J. and Venkatasubramanian, V.M. (2007) Oscillation Monitoring System Based on Wide Area Synchrophasors in Power Systems. 2007 *iREP Symposium on Bulk Power System Dynamics and Control, VII. Revitalizing Operational Reliability*, Charleston, SC, 19-24 August 2007, 1-13. <http://ieeexplore.ieee.org/stamp/stamp.jsp?arnumber=4410548>
- [12] Wai, D.C.T. and Xia, Y. (1998) A Novel Technique for High Impedance Fault Identification. *IEEE Transactions on Power Delivery*, **13**, 738-744. <http://ieeexplore.ieee.org/stamp/stamp.jsp?arnumber=686968>
<https://doi.org/10.1109/61.686968>
- [13] Girgis, A., Chang, W. and Makram, E.B. (1990) Analysis of High-Impedance Fault Generated Signals Using a Kalman Filtering Approach. *IEEE Transactions on Power Delivery*, **5**, 1714-1724. <https://doi.org/10.1109/61.103666>
<http://ieeexplore.ieee.org/stamp/stamp.jsp?arnumber=103666>
- [14] Huang, S.-J. and Hsieh, C.-T. (1999) High Impedance Fault Detection Utilizing Morlet Wavelet Transform Approach. *IEEE Transactions on Power Delivery*, **14**, 1401-1410. <http://ieeexplore.ieee.org/stamp/stamp.jsp?arnumber=796234>
<https://doi.org/10.1109/61.796234>
- [15] Lai, T.M., *et al.* (2005) High-Impedance Fault Detection Using Discrete Wavelet Transform and Frequency Range and RMS Conversion. *IEEE Transactions on Power Delivery*, **20**, 397-407. <https://doi.org/10.1109/TPWRD.2004.837836>
<http://ieeexplore.ieee.org/stamp/stamp.jsp?arnumber=1375120>
- [16] Sedighi, A.-R., *et al.* (2005) High Impedance Fault Detection Based on Wavelet Transform and Statistical Pattern Recognition. *IEEE Transactions on Power Delivery*, **20**, 2414-2421. <http://ieeexplore.ieee.org/stamp/stamp.jsp?arnumber=1514486>
<https://doi.org/10.1109/tpwr.2005.852367>
- [17] Ece, D.G. and Gerek, O.N. (2004) Power Quality Event Detection Using Joint 2-D-Wavelet Subspaces. *IEEE Transactions on Instrumentation and Measurement*, **53**, 1040-1046. <http://ieeexplore.ieee.org/stamp/stamp.jsp?arnumber=1315981>
<https://doi.org/10.1109/tim.2004.831137>

Submit or recommend next manuscript to SCIRP and we will provide best service for you:

Accepting pre-submission inquiries through Email, Facebook, LinkedIn, Twitter, etc.

A wide selection of journals (inclusive of 9 subjects, more than 200 journals)

Providing 24-hour high-quality service

User-friendly online submission system

Fair and swift peer-review system

Efficient typesetting and proofreading procedure

Display of the result of downloads and visits, as well as the number of cited articles

Maximum dissemination of your research work

Submit your manuscript at: <http://papersubmission.scirp.org/>

Or contact jpee@scirp.org